Metamorphic history of the Hemlo gold deposit from Al$_2$SiO$_5$ mineral assemblages, with implications for the timing of mineralization

Wayne G. Powell, David R.M. Pattison, and Paul Johnston

Abstract: Textural relations between Al$_2$SiO$_5$ phases, and deformation fabrics, provide constraints on the metamorphic history of the Hemlo gold deposit. Kyanite in the deposit is most common within and on the margins of boudinaged quartz ± realgar veins, and less commonly as rotated porphyroblasts within the matrix of schistose rocks. Kyanite predates the main (D2) schistosity. Sillimanite postdates kyanite, occurring irregularly as discrete knots and foliae that run parallel to, but sometimes cut across, the principal (D2) foliation, indicating that sillimanite postdates the D2 foliation. We regard kyanite to be part of the peak metamorphic assemblage, with sillimanite representing a partial later overprint most likely related to fluid infiltration. Rare andalusite occurs in two associations: as late-stage, clean, idioblastic crystals; and as large, fractured grains, locally overprinted by sillimanite, in boudinaged quartz–realgar veins. We suggest two possible origins for this second form of andalusite, one involving generally late growth, the second involving early growth prior to the development of peak metamorphic kyanite. Although not unambiguous, we prefer the second scenario. P–T conditions from petrogenetic grid constraints, and new geothermobarometric estimates, indicate 6–7 GPa, 600–650°C for the peak kyanite grade metamorphism (ca. 2677 Ma?), and 4–5 GPa, 600°C for the later sillimanite overprint (ca. 2672 Ma?). We see these two events as part of an evolving P–T path in a single metamorphic event. In our early andalusite scenario, the andalusite may have formed from pyrophyllite breakdown at 2–4 GPa, 450°C, possibly associated with emplacement of the regional suite of granodiorite plutons (ca. 2686 Ma). Late andalusite formed sporadically on the retrograde path. The occurrence of deformed andalusite and aligned kyanite in and on the margins of boudinaged auriferous realgar–stibnite–quartz veins provides evidence in support of a premetamorphic mineralization event.

Résumé : Les relations texturales entre les phases de Al$_2$SiO$_5$, et la fabrique de déformation, fournissent des contraintes pour ce qui est de l'interprétation de l'histoire métamorphique du gisement de Hemlo. La kyanite (disthène) dans le gisement est rencontrée le plus communément à l'intérieur et sur les bordures des filons boudinés de quartz ± réalgar, et moins fréquemment sous forme de porphyroblastes ayant subi une rotation dans la matrice des roches schisteuses. La sillimanite qui postdate la kyanite apparaît irrégulièrement sous l'aspect de petits noeuds foliés disposés parallèlement à la foliation principale (D2), parfois la recoupant, ce qui signifie que la sillimanite postdate la foliation D2. Nous considérons que la kyanite fait partie de l'assemblage métamorphique culminant, et dont la sillimanite représente une cristallisation partielle plus tardive probablement associée à l'infiltration des fluides. On peut observer exceptionnellement l'andalousite dans deux types d'association : l'une étant de stade tardif, sous forme de cristaux idioblastiques clairs; l'autre avec de gros grains fracturés et localement recouverts de sillimanite dans les filons boudinés de quartz–réalgar. Nous proposons pour cette seconde forme d'andalousite deux origines possibles, une impliquant généralement une croissance tardive, l'autre comprenant plutôt une croissance précoce antérieure à l'apparition de la kyanite lors de l'apogée métamorphique. Nous optons de préférence pour la seconde hypothèse, bien qu'elle ne soit pas sans ambiguïtés. Les conditions culminantes de P–T pour le métamorphisme allié à la kyanite, déduites d'une grille de contraintes pétrogénétiques et d'estimations géothermobarométriques étaient de 6–7 GPa et 600–650°C (vers 2677 Ma?), et lors de la surimpression de sillimanite plus tardive (vers 2672 Ma?) elles étaient de 4–5 GPa et 600°C. Nous croyons que ces deux événements faisaient partie d'un chemin P–T évoluant au sein d'un crise métamorphique unique. Si notre hypothèse d'une cristallisation précoce de l'andalousite est correcte, ce minéral aurait été formé à partir de la destruction de la pyrophyllite à 2–4 GPa et 450°C, probablement associée à la mise en place de la suite régionale des plutons de granodiorite (vers 2686 Ma). L'andalousite tardive a cristallisé de manière sporadique par rétrométamorphisme. La présence d'andalousite déformée et l'alignement des cristaux de kyanite dans et sur les bordures des filons de réalgar–stibine–quartz aurifères, plaident en faveur d'un événement antémétamorphique.

[Traduit par la Rédaction]

W.G. Powell[1] **and D.R.M. Pattison.** Department of Geology and Geophysics, The University of Calgary, Calgary, AB T2N 1N4, Canada.

P. Johnston. Teck Exploration Ltd., Southeast Asia Representative Office, 268 Orchard Road, 16-01 Yen San Building, Singapore 238856.

[1]Corresponding author (powell@geo.ucalgary.ca).

Introduction

The timing of mineralization at the Hemlo gold deposit is controversial (e.g., Fleet and Pan 1995; Kuhns et al. 1995), largely due to the structural–metamorphic complexity of this deposit and an inability to date the gold directly. In its simplest terms, this debate commonly focuses on the age of gold mineralization relative to regional metamorphism: did gold mineralization occur before (e.g., Kuhns et al. 1994, 1995), during, or after (e.g., Pan and Fleet 1995) regional metamorphism? In addition to its scientific interest, this question carries significant implications for exploration strategies for other Hemlo-like deposits.

Recent studies of other gold deposits from the Superior Province (e.g., Couture et al. 1994) have shown that different deposits may have formed at different times with respect to metamorphism. Age determinations from dykes that crosscut mineralization have demonstrated a premetamorphic age for some Archean gold deposits (Couture et al. 1994; Morasse et al. 1995). Other researchers provide convincing arguments for postmetamorphic mineralization (e.g., Robert and Brown 1986). The interpretation of the relative timing of mineralization is often complicated by the fact that most Archean gold deposits, including Hemlo, have experienced complex histories of metamorphism, deformation, and hydrothermal activity. Later hydrothermal events may create overprinting metamorphic and metasomatic mineral assemblages, reset isotopic systems, and introduce several generations of fluid inclusions. Nevertheless, careful examination of mineral assemblages and textures can help reconstruct the metamorphic history and provide insights into the relative timing of metamorphism, mineralization, and alteration.

In this paper, we use textural relationships to determine the relative timing of Al_2SiO_5 minerals (kyanite, sillimanite, andalusite) that developed in aluminous rocks associated with the Hemlo deposit. Combinations of all three Al_2SiO_5 polymorphs, along with other aluminous minerals such as staurolite and garnet, occur in the altered rocks within and surrounding the deposit. Our interpretation of these mineral assemblages provides constraints on the metamorphic history of the deposit and, although it is not the focus of this paper, carries implications for the regional metamorphic history of the belt. Our findings also bear on the debate over the timing of Au mineralization with respect to metamorphism.

Geology of the Hemlo deposit and vicinity

Since production began in 1985, the three mines that exploit the Hemlo gold deposit (Williams mine, Golden Giant mine, and David Bell mine) have produced 9.5 million ounces of gold and account for one quarter of Canada's gold production. This deposit is located in the late Archean Schreiber–Hemlo greenstone belt (Wawa Subprovince, Superior Province) of northwestern Ontario. Williams et al. (1991) provide an overview of regional geology of the Wawa subprovince, including the Schrieber–Hemlo greenstone belt.

The Hemlo deposit is situated in a linear zone of particularly strong deformation that trends parallel to the general west-northwest–east-southeast structural trend of the area.

This deformation zone is locally termed the Hemlo shear zone. The Proterozoic Port Coldwell alkalic complex, which divides the belt into two segments, marks the western extent of the Hemlo shear zone. Based on discontinuous outcrops, this band of deformation is interpreted to extend eastward across the length of the greenstone belt, and beyond into the surrounding granitoids (Williams et al. 1991).

Several researchers have documented the multiply deformed nature of the Schreiber–Hemlo greenstone belt, particularly in the immediate mine area (e.g., Muir 1997; Michibayashi 1995; Kuhns et al. 1994). In the mine area, the strata generally strike west-northwest–east-southeast and dip steeply north. The earliest recognized structural elements are isoclinal folds associated with a bedding-parallel foliation (F1 of Kuhns et al. 1994). These folds are premetamorphic. The predominant structural element in the Hemlo area is a set of large-scale, east–west- to west-northwest–east-southeast-trending, shallowly plunging isoclinal folds with a strong axial planar cleavage (F2a and S2a of Kuhns et al. 1994). Kuhns et al. (1994) argued that F2a locally folds ore. These folds are parallel to the margin of the Pukaskwa batholith that marks the southern boundary of the greenstone belt. Small dextral folds (F2b of Kuhns et al. 1994) affect the predominant axial-planar cleavage (S2a). This dextral-shear event developed late in the metamorphic history, and locally folded and boudinaged ore-cutting porphyry dykes (Kuhns et al. 1994). Northwest-striking brittle faults with dextral displacement are associated with overprinting greenschist-facies retrograde mineral assemblages (Kuhns et al. 1994).

The main ore zone lies within a highly deformed sequence of metasedimentary and metavolcanic strata (see detailed descriptions of Muir 1993 and Kuhns et al. 1994), adjacent to the highly deformed Moose Lake quartz–feldspar porphyry complex (Fig. 1). U/Pb dating of zircon from a felsic fragmental rock from the immediate mine area, interpreted to be a metavolcanic unit, yielded an age of 2772 ± 2 Ma (Corfu and Muir 1989a). Zircons from a volcanic rock located near Heron Bay yielded a U/Pb age of 2695 ± 2 Ma (Corfu and Muir 1989b) volcanic. Published dates are not available for the Moose Lake porphyry, but this intrusion is cut by felsic dykes that contain zircons dated at 2680–2690 Ma (U/Pb) (Kuhns et al. 1994). Granodiorite–diorite plutons and associated dykes (Kuhns et al. 1994) intruded the supracrustal rocks in the belt between 2690 and 2678 Ma (U/Pb dating of zircon, Corfu and Muir 1989a). Kuhns et al. (1994) argued that porphyry dykes that cut the ore zone and associated alteration are petrologically and geochemically very similar to the dated dykes, supporting Muir's (1993) suggestion that the dated felsic dykes place a minimum age on the mineralization.

Mineralization and alteration

In the Hemlo deposit, gold is spatially associated with altered rocks that are composed primarily of Ba-rich microcline (Johnston 1996; Harris 1989). Gold grades correlate directly with Mo grades. In general, the deposit is also enriched in Sb, As, Hg, Tl, Ba, V, and B (Harris 1989). However, metals are broadly zoned across the deposit. As, Hg, and Tl occur in the central part of the deposit, but these

Fig. 1. General geology of the Hemlo – Heron Bay greenstone belt. Modified from Kuhns et al. (1994).
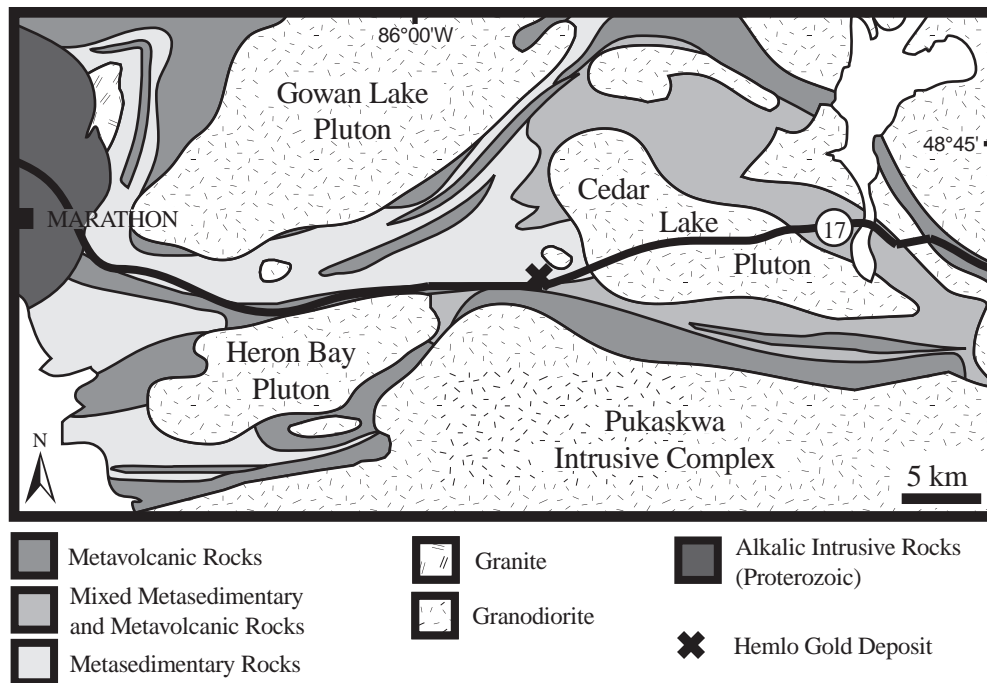
metals are near absent from the northwest downplunge extension of the Williams mine, where there is an increased abundance of the base metal minerals galena, chalcopyrite, and sphalerite (Harris 1989). The sulphide phases at the Hemlo deposit exhibit complex textures and show evidence of sequential exsolution of lower-temperature minerals, such as realgar, orpiment, and cinnabar (Powell and Pattison 1997).

Alteration zones associated with the ore zone are spatially associated with the Moose Lake porphyry complex (Johnston 1996) (Fig. 2). The core of the Moose Lake porphyry has been intensely sericitized, and subsequently deformed, forming a quartz-eye schist in which quartz phenocrysts occur in a schistose matrix of sericite, muscovite, and fine-grained quartz. The ore zones and their associated intense microcline alteration occur outboard of the sericite alteration. A more extensive zone of weakly feldspathic alteration, characterized by purple-brown, weakly feldspathic metasedimentary rocks, occurs outside of the microcline zone (Johnston 1996). These weakly feldspathized rocks also are rather aluminous, as revealed by the common occurrence of kyanite, sillimanite, staurolite, and garnet which are more abundant in these rocks than in the country rocks away from the deposit (Johnston 1996; Kuhns 1986; Walford et al. 1986).

Kuhns et al. (1994) and Johnston (1996) argued that these aluminous rocks represent the metamorphosed equivalent of a distal zone of aluminous, possibly argillic, alteration that surrounded the deposit. In contrast, it has been proposed that these aluminous rocks are simply metapelitic rocks, with no genetic association with the deposit (Fleet et al. 1997).

We note that within the deposit the aluminous minerals kyanite, staurolite, and garnet are most common within deformed veins and veinlets, rather than within the rock matrix. Furthermore, fibrolitic sillimanite is most common in the selvages of these aluminous veinlets. If the veins originally were clay-bearing, or had aluminous alteration selvages (e.g., argillic or phyllic alteration selvages, as is common in veins from many unmetamorphosed magmatic hydrothermal systems), the aluminous metamorphic minerals now associated with the veins may simply represent metamorphosed alteration assemblages. In addition, kyanite occurs not only within altered metasedimentary rocks, but also within altered Moose Lake porphyry. Thus, the above associations provide support in favour of an alteration origin for at least some of the aluminous rocks, although we do not rule out the possibility that some of the aluminous rocks, particularly outside of the deposit, may be pelitic metasedimentary rocks.

Pan and Fleet (1992, 1995) argued that the alteration postdated regional metamorphism. Kuhns et al. (1994) and Johnston (1996) noted that all of the ore-associated alteration zones are foliated and folded (F2a and S2a events of Kuhns et al. 1994), and contain metamorphic minerals indicative of amphibolite-facies metamorphic events (see below). This implies that the alteration predated, or was synchronous with, regional metamorphism and deformation. This inference does not extend to obviously later alteration types (see Pan and Fleet 1992, 1995) that affected the rocks of the belt.

Metamorphism

Belt-scale studies of the regional metamorphic history have not been completed. Work in progress indicates that metamorphic grade increases both from west to east, and approaching both internal and bounding granitoid bodies (Jackson 1997). In rocks of metapelitic composition, away from plutons, assemblages progress from garnet–chlorite in the east to garnet–biotite–sillimanite in the west (Jackson 1997). Pan and Fleet (1993) suggested that metamorphic grade also increases within zones of increased deformation.

Fig. 2. Map of alteration zones relative to the Moose Lake porphyry. Modified from Johnston (1986).
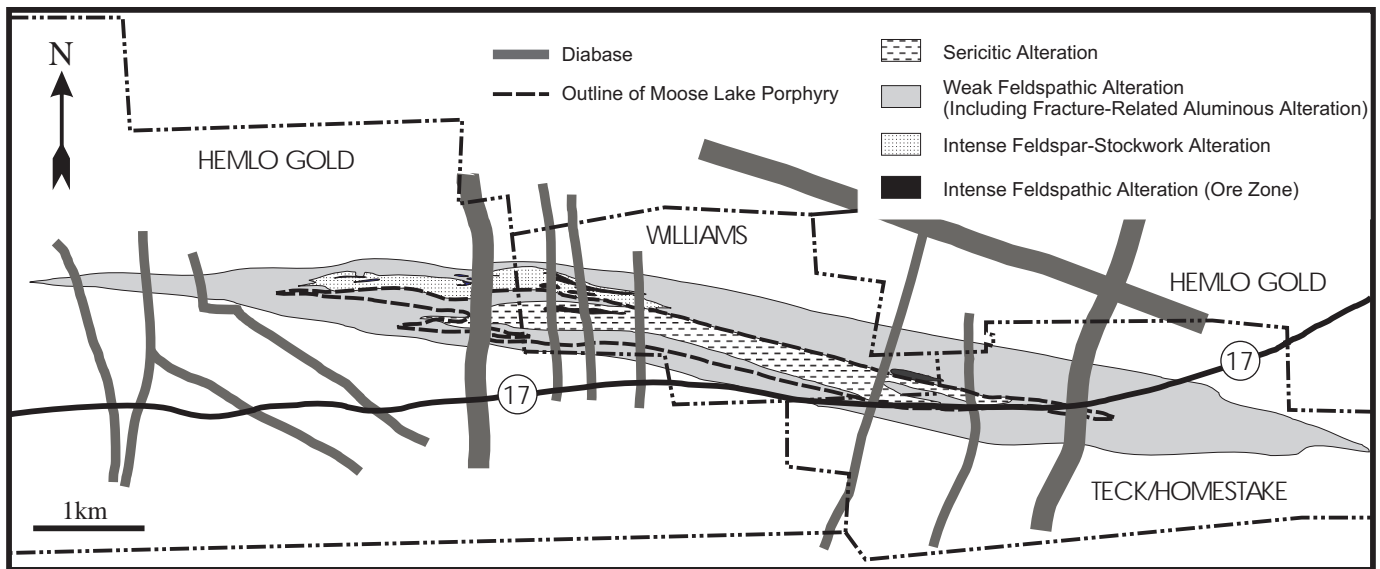
Three detailed studies of the metamorphic history of parts of the Schreiber–Hemlo greenstone belt, including the Hemlo deposit, have been published: Burk et al. (1986) and Kuhns et al. (1994) studied the metamorphism of the deposit and its immediate vicinity, whereas Pan and Fleet (1993) studied the White River property, located 5–10 km east of the Hemlo deposit. Owing to the aforementioned west–east metamorphic gradient in the belt, this spatial separation raises some uncertainty in the following discussion comparing the studies (i.e., the metamorphic evolution may have been different in the two different localities).

The three sets of authors proposed rather different interpretations of the timing and character of the regional metamorphism, but agree on the following two points:

(1) A moderate-pressure metamorphic mineral assemblage (M1), characterized by the assemblage Ky–St–Grt–Bt–Ms–Pl–Qtz in aluminous rocks, predates a lower-pressure, over-printing metamorphic mineral assemblage (M2) characterized by the assemblage Sil–Grt–Bt–Ms–Pl–Qtz (abbreviations of Kretz 1983).

(2) Estimates of metamorphic conditions for the moderate-pressure M1 mineral assemblage vary between 6 GPa and 500°C (Pan and Fleet 1993) to 6–8 GPa and 600°C (Burk et al. 1986; Kuhns et al. 1994). However, all agree on 4–5 GPa and 600°C for conditions attending sillimanite growth (M2).

The relationship between the earlier moderate-pressure M1 (Ky–St) and the later lower-pressure M2 (Sil) growth events is debated, with the debate focusing on whether the two mineral assemblages represent two discrete metamorphic events or different stages in a single metamorphic event. Burk et al. (1986) interpreted the kyanite assemblage to have developed at the peak of a single metamorphic event, followed by sillimanite growth on the retrograde path during more or less isothermal uplift, a view generally supported by Kuhns et al. (1994). In contrast, Pan and Fleet (1993) proposed two distinct metamorphic events, with the higher-temperature, lower-pressure sillimanite event (M2, part of an andalusite–sillimanite-type sequence according to Pan and Fleet 1995; Fleet and Pan 1995) superimposed on an earlier

lower-temperature, higher-pressure kyanite-grade assemblage (M1).

The relative timing of metamorphic mineral growth relative to deformation events is also debated. Burk et al. (1986) and Pan and Fleet (1993) both interpreted fibrolitic sillimanite growth (M2) to be synchronous with the development of the dominant foliation (F2a of Kuhns et al. 1994), whereas kyanite-bearing assemblages developed prior to this tectonic event. In contrast, Kuhns et al. (1994) suggested that development of the earlier M1 kyanite–staurolite-bearing assemblages was coeval with regional F2a schistosity development, and the later sillimanite-bearing assemblages postdated any significant ductile deformation.

Absolute timing of metamorphism

U/Pb dating of titanite (closure temperature approximately 600–700°C; Heaman and Parrish 1991; Scott and St-Onge 1995) from unmineralized rock near the deposit suggests that peak M1 metamorphism occurred at ca. 2678–2676 Ma (overlap of titanite ages; Corfu and Muir 1989b). Titanite from within the deposit, commonly associated with postpeak metamorphic mineral assemblages (Kuhns et al. 1994, their M2) yielded younger U/Pb ages of 2672–2670 ± 3 Ma (Corfu and Muir 1989b). Protracted cooling of the deposit is suggested by $^{40}Ar/^{39}Ar$ dating of hornblende (closure approx. 550°C, ca. 2645 Ma), muscovite (closure approx. 350°C, ca. 2615 Ma), and biotite (closure approx. 280°C, ca. 2570 Ma) from upper levels of the mines (Grant 1995).

Pan and Fleet (1993) interpreted the M2 sillimanite-bearing assemblages to have grown during the intrusion of the granodioritic Cedar Lake pluton (2688–2684 Ma, U/Pb zircon; Corfu and Muir 1989a), implying that the M1 Ky–St assemblages predated the Cedar Lake pluton. In contrast, Kuhns et al. (1994) interpreted the M1 kyanite–staurolite-bearing assemblages to have grown during intrusion of the Cedar Lake pluton, and speculated that M2 sillimanite growth corresponded to the 2672–2670 Ma event of Corfu and Muir (1989b). The latter case is supported by the development of weak to moderate fabric development along the margin of the Cedar Lake stock, as well as a weak foliation

within this pluton which is parallel to the predominant regional foliation (Jackson 1997; Muir 1997).

Distribution and description of Al₂SiO₅-bearing rocks in the deposit

Distribution of Al₂SiO₅ minerals in the vicinity of the Hemlo deposit

Although sillimanite is fairly widely distributed in regional metasedimentary rocks near the Hemlo deposit and elsewhere in the belt (S.L. Jackson, personal communication, 1998), in general aluminosilicate minerals are more abundant and more diverse in the immediate vicinity of the deposit. The limit of abundant Al_2SiO_5-bearing assemblages defines the farthest extent of weakly feldspathically altered aluminous rocks which lies adjacent to the Moose Lake porphyry and the associated ore zones.

Aluminous minerals (sillimanite, kyanite, garnet, staurolite, and rare andalusite) are particularly abundant within the eastern portion of the feldspathically altered aluminous rocks, and appear to show a zonal distribution (Fig. 3) (Johnston 1996). Kyanite, sillimanite, staurolite, and garnet occur within a broad outer zone (up to 350 m wide) of purple-brown, weakly feldspathized metasedimentary rocks, in which they are most commonly associated with deformed veinlets and their selvages (Johnston 1996). Within the inner, more highly feldspathized zone, kyanite and sillimanite are abundant, whereas staurolite and garnet are minor phases. Kyanite and sillimanite without garnet and staurolite occur in the most intensely altered portions of the inner feldspathized zone (Johnston 1996). Kyanite and sillimanite also occur in deformed quartz veinlets within sericiticly altered quartz–feldspar porphyry. Andalusite is a rare and sporadically distributed mineral within the aluminous rocks.

Kyanite

Kyanite is the most conspicuous Al_2SiO_5 polymorph within the alteration zones at Hemlo (Kuhns et al. 1994). It most commonly occurs as subhedral, commonly poikiloblastic, grains within thin (<2 mm wide), foliation-parallel veinlets (Fig. 3A) that are commonly folded. Kyanite grains lie parallel to the vein margins. The mineral assemblages within the veinlets vary, and include Ky–St–Bt–Qtz (Fig. 3B), St–Bt–Qtz, Grt–Bt–Qtz, and Ky–Bt–Qtz. Retrograde chlorite and muscovite occurs in most Ky-bearing veins, but the kyanite grains themselves are rarely sericitized. In muscovite-rich rocks, kyanite grains commonly display evidence of rotation in the plane of the main foliation.

At the contact between the ore zone and hanging-wall metasedimentary rocks of the David Bell mine, parallel blades of coarse (5 cm long) kyanite encrust boudins of a realgar–stibnite-bearing quartz vein. The crystals are euhedral to subhedral, generally unaltered, but some grains are overgrown by fibrolitic sillimanite. Some corroded kyanite grains occur within these quartz boudins, encased within highly sericitized andalusite.

A similar texture of kyanite relics encased in deformed, sericitized andalusite occurs in a large quartz pod from the surface pit of the Williams mine. A thin, discontinuous alter-ation rim of tourmaline, biotite, kyanite, and staurolite borders this quartz pod. The staurolite and kyanite in the selvages show no evidence of overgrowth or retrogression.

Sillimanite

Sillimanite is a relatively common phase in the western end of the Schrieber–Hemlo greenstone belt (Pan and Fleet 1993; S.L. Jackson, personal communication, 1997), but is more abundant in close proximity to the ore zones (Kuhns et al. 1994). Within the deposit, it occurs as fibrolite (see Kerrick 1990, pp. 207–220; and Pattison 1992, pp. 424–426, for a discussion of the distinction between fibrolite and prismatic sillimanite). A significant feature of the sillimanite in the deposit, also noted by Kuhns et al. (1994), is that it is nonuniformly distributed throughout the matrix of the rocks, instead occurring in discrete knots and foliae. Although these fibrolitic concentrations are generally aligned parallel to the dominant foliation, they commonly anastamose across the foliation (Fig. 3C). Within the segregations, most sillimanite needles lie approximately parallel to the foliation, but many needles radiate at high angles to the schistosity and are undeformed (Fig. 3C) (see also Fig. 7d of Kuhns et al. 1994).

Sillimanite is more abundant in rocks that include biotite in the matrix, and commonly it is intergrown with, and appears to replace, the biotite (e.g., Fig. 7e of Kuhns et al. 1994). Sillimanite only occurs in rocks that are muscovite bearing, wherein sillimanite knots are usually associated with a narrow halo of muscovite depletion. Sillimanite also commonly occurs along the margins of deformed kyanite-bearing veinlets.

Kyanite and sillimanite are rarely found in direct contact. Typically, fibrolite knots occur in the micaceous host rock, adjacent to Ky ± St ± And-bearing quartz veinlets. Although sillimanite does not directly replace the other aluminosilicate polymorphs, fibrolite needles crosscut both kyanite and andalusite grain margins.
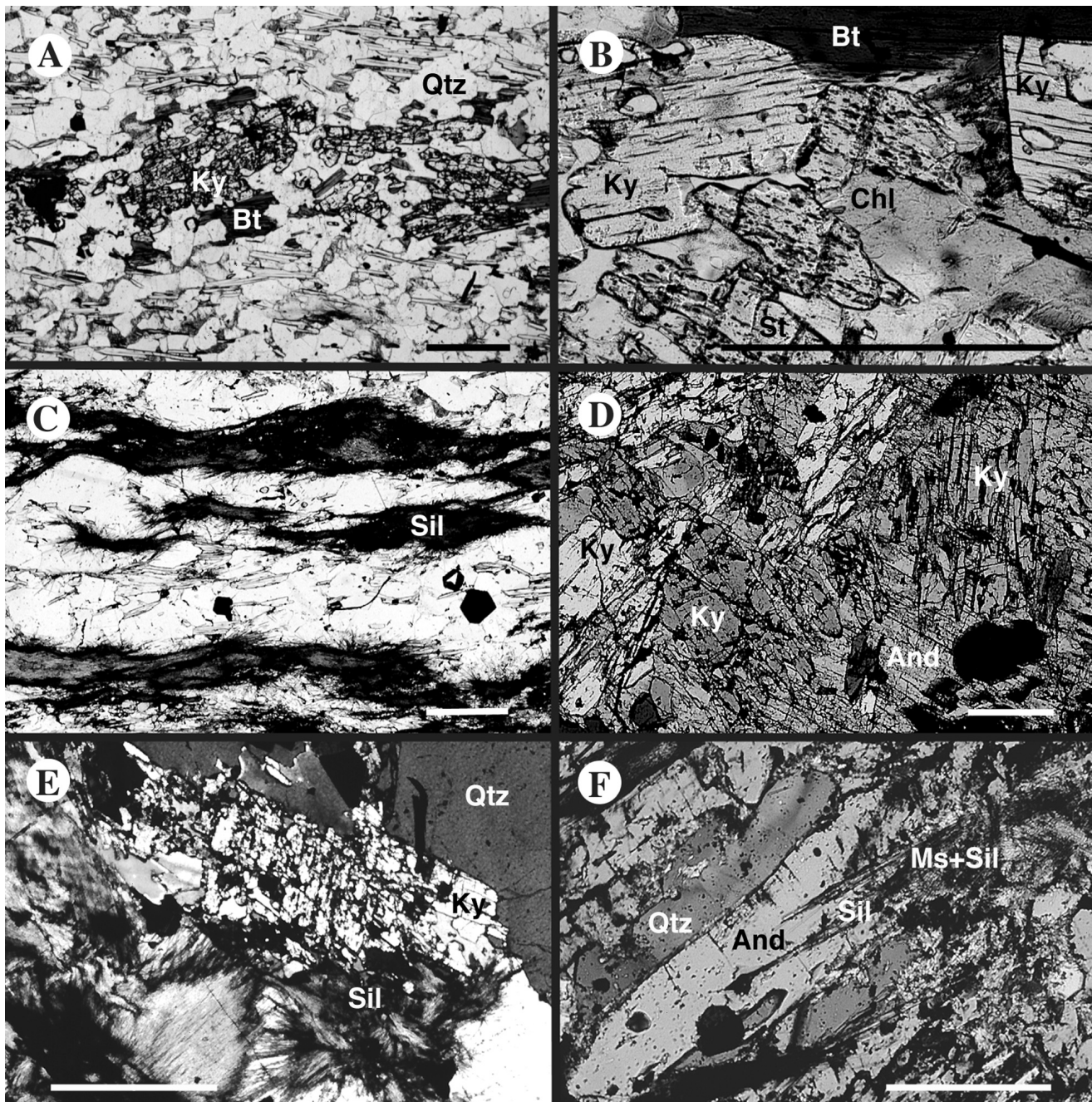
Andalusite

Andalusite is the least abundant of the aluminosilicate polymorphs within the Hemlo deposit, and occurs in two main textural and lithological associations. It rarely occurs as small, unaltered, idioblastic crystals in biotite-rich rocks in the main ore zone of the Golden Giant mine (Fig. 7f of Kuhns et al. 1994). This form of andalusite we term And2.

The more common variety occurs within deformed quartz veins, including boudinaged realgar-bearing veins, which we term And1. Vein-associated andalusite occurs as large (0.5–2 cm) anhedral to subhedral grains that are commonly poikiloblastic, with inclusions of quartz and kyanite. The kyanite inclusions are anhedral to subhedral and generally corroded (Fig. 3D). Sets of isolated kyanite inclusions (in two dimensions) that are in optical continuity are enclosed within these andalusite crystals. A few vein-associated andalusite grains are crosscut by fine-grained sillimanite needles.

The vein-associated andalusite grains commonly display undulose extinction and are fractured. Coarse muscovite and sericite are ubiquitous alteration phases along fractures and rims. Sericite most commonly occurs as felted mats, whereas replacement muscovite forms large, sometimes skeletal, grains that enclose remnants of andalusite. This

Fig. 3. Mineral textures and associations in photomicrographs. (A) Annealed Ky–Bt–Qtz veinlets in Kf–Qtz–Ms schist. (B) Ky–St–Bt–Qtz within a quartz pod. Chl is retrograde. (C) Anastamosing fibrolitic sillimanite. Note that although pods are subparallel to the foliation planes, many needles are at a high angle to the foliation. (D) Corroded kyanite inclusions within andalusite. (E) Fibrolitic sillimanite overgrowing kyanite. (F) Fibrolitic sillimanite overgrowing andalusite. Scale bars = 0.5 mm.

coarse muscovite replacement texture is only seen with andalusite, and contrasts with the fine-grained sericite that also replaces andalusite and, to a lesser extent, kyanite. In andalusite grains showing both types of alteration, the coarse replacement muscovite appears to predate the sericite.

Metamorphic history of the Hemlo deposit deduced from Al_2SiO_5 relations

In this section, we attempt to construct a metamorphic history that reconciles the textures of the Al_2SiO_5 poly-

morphs and speculate on possible ages for the different Al_2SiO_5-producing events. This information is combined with P–T estimates to allow construction of possible P–T–time paths for the metamorphism (Fig. 4).

Interpretation and timing of sillimanite

Within rocks containing sillimanite and kyanite, the sillimanite is always later than the kyanite, as evidenced by fibrolitic needles growing across the margins of the kyanite (Fig. 3E). However, the sillimanite does not appear to actually replace kyanite. In all Sil-bearing rocks we observed, al-

Fig. 4. (A) Petrogenetic grid for metapelitic-like rocks containing Ms + Qtz + Bt (solid lines), modified from Pattison and Tracy (1991) (see text and Pattison and Tracy 1991, pp. 165–170, for details of construction). Dashed reactions are for unusually aluminous compositions. –Mn and +Mn refer to the position of reaction [2] for Mn-free and Mn-bearing garnet, respectively, resulting in a band (shaded region) (see text for discussion). (B) Previous P–T paths of the Hemlo deposit and belt. BHQ, Burk et al. 1986; KSI, Kuhns et al. 1994; PF M1, M1 event of Pan and Fleet 1993; PF M2, M2 event of Pan and Fleet. The two black ellipses are recalculated P–T results (TWQ, Berman 1991; Berman and Aranovich 1996 data set) for the Burk et al. (1986) data (see text for discussion). (C) Inferred P–T path for our andalusite scenario 1 (see text for discussion). The solid dots represent the inferred P–T conditions and relative timing of growth of the different textural varieties of the Al$_2$SiO$_5$ minerals. (D) Inferred P–T path for our andalusite scenario 2 (see text for discussion).
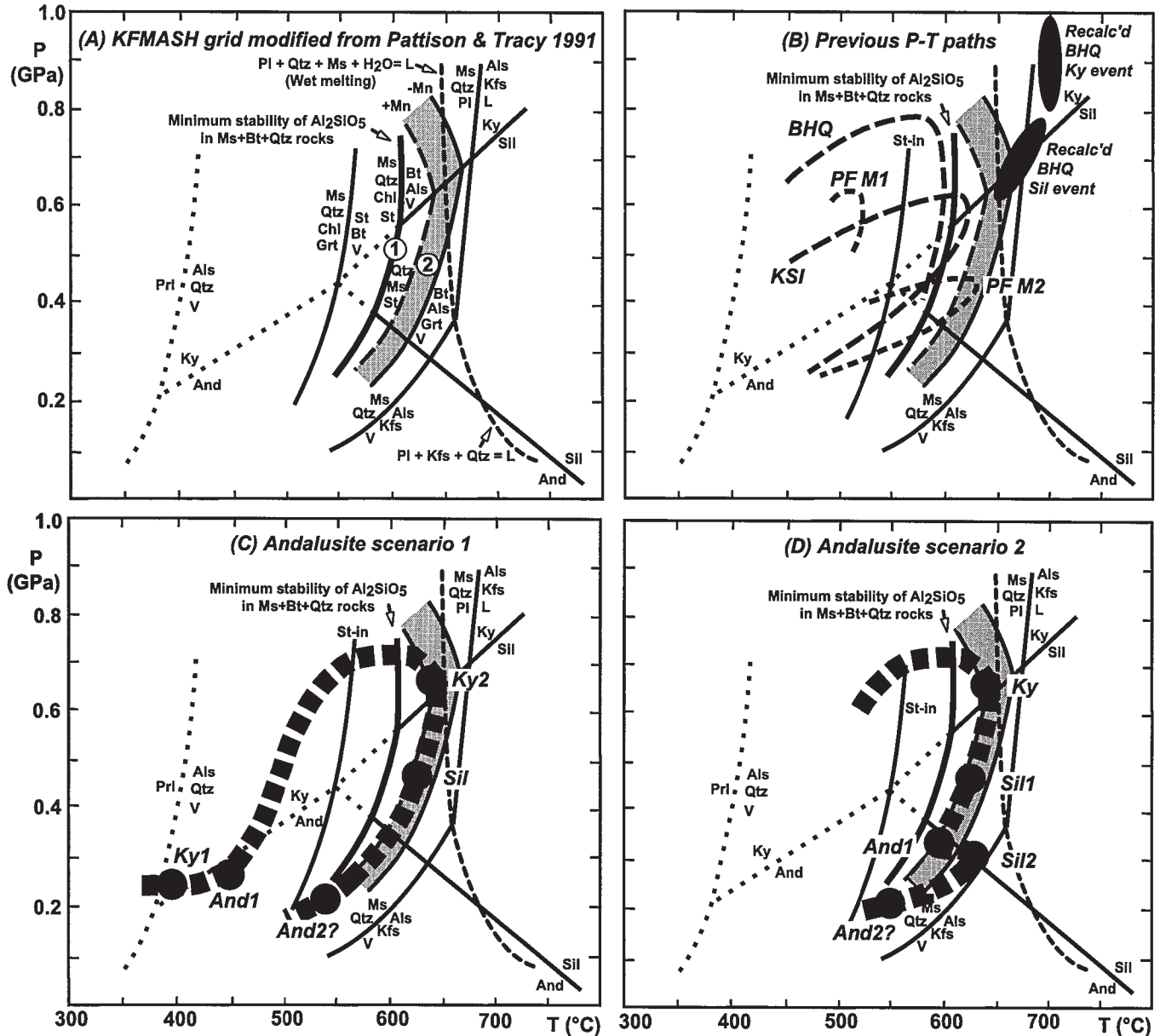
though the fibrolite bundles lie along the foliation planes, individual needles are randomly oriented and crosscut the foliation without any evidence of deformation despite their delicate nature. Accordingly, sillimanite growth is interpreted to have largely postdated the development of the dominant regional foliation, as previously suggested by Kuhns et al. (1994).

The irregular and anastamosing distribution of fibrolite knots along and across the foliation, and its conspicuous re-

placement association with preexisting biotite crystals, raises uncertainty as to whether it should be treated as a stable phase in equilibrium with the rest of the minerals in the host rock. This style of sillimanite occurrence has been reported widely elsewhere (see review in Kerrick 1990, pp. 243–253, 273–296, 346–352). Kerrick (1990) and most other authors referenced in his review interpreted formation of this type of sillimanite to have been controlled by catalytic and (or) metasomatic effects associated with localized fluid migra-

tion along discrete conduits. At Hemlo, the conduits appear to have been cleavage planes and vein margins.

The proposed sillimanite-producing reactions range from base cation leaching of micas or feldspar (Vernon 1979), in which infiltrating acid fluids leach Fe, Mg, and alkalies from the micas or feldspar and leave behind an Al_2SiO_5-rich residue; pressure-induced dissolution of micas and feldspars (Wintsch and Andrews 1988), leaving behind an Al_2SiO_5-rich residue (similar to base cation leaching, only involving less fluid); reduction in aH_2O or $aK+$ in the fluid, leading to destabilization of muscovite or pyrophyllite (Eugster 1970); and a variety of mechanisms involving metasomatic introduction of Al and other elements to the sites of fibrolitic sillimanite growth (Kerrick 1990). In these scenarios, the suggested origins of the metasomatizing fluids range from magmatic fluids given off from crystallizing intrusions to metamorphic fluids derived from elsewhere (generally deeper) in the metamorphic pile, to locally produced metamorphic fluids within the sillimanite-bearing rocks. In most of the studies reviewed by Kerrick (1990), this type of sillimanite was interpreted to be separate from and later than the peak metamorphic assemblage, a view which we feel applies to Hemlo as well.

Thus, we agree with the view of Kuhns et al. (1994) that the textures of fibrolitic sillimanite at Hemlo are most consistent with growth during late fluid-associated recrystallization following peak metamorphism (Figs. 4B, 4C), rather than growth as a stable phase in equilibrium with the rest of the rock during prograde metamorphism as suggested by Burk et al. (1986). This interpretation also differs from that of Pan and Fleet (1993), although we note again that their study area lies 5–10 km east of the deposit. Regarding the $P–T$ conditions of sillimanite growth, we feel that it is unlikely that the temperature was significantly lower than that of peak conditions (although the pressure must have been somewhat lower), owing to the general agreement in $P–T$ estimation for the sillimanite growth in all three previous studies (see above) which suggests that mineral compositions may have reequilibrated during this episode. Thus, it is a moot point whether this growth episode should be described as retrograde.

An unconstrained aspect of this interpretation is the origin and age of the fluid infiltration. Regarding the age, Kuhns et al. (1994) made analogous textural arguments pertaining to localized development of radiating clusters of actinolite–tremolite crystals that crosscut the main foliation and tremolitic–actinolitic-hornblende rims on earlier hornblende crystals, in metabasaltic rocks within, and in close proximity to, the ore zone. They argued that the tremolitic–actinolitic amphiboles represented a late, relatively static overprint (M2) on the peak metamorphic hornblende assemblage (M1), and correlated this growth with the development of fibrolitic sillimanite. All that can be really concluded is that sillimanite and late amphibole formation both postdated the main deformation events. Kuhns et al. observed titanite to be intergrown with the late tremolitic–actinolitic amphibole, and thus suggested that the titanite U/Pb date of 2672 ± 3 Ma from within the deposit (Corfu and Muir 1989b) may reflect their late sillimanite and tremolite–actinolite recrystallization event. Based on the stability ranges of tremolite–actinolite, actinolitic hornblende (actinolite-out

approx. 530°C, Begin 1992) and sillimanite (sillimanite-in approx. >580°C; Fig. 4), it is likely that the late amphibole replacement occurred at lower temperature, and therefore later than the sillimanite. Accordingly, the 2672 Ma titanite date should be considered a minimum age for sillimanite growth.

Interpretation and timing of kyanite

In the samples we observed, kyanite occurs most commonly within foliation-parallel quartz-rich veinlets, in the selvages of boudinaged quartz veins, and in deformed quartz pods. Because of this isolation of kyanite from the schistose host rock, the relationship of kyanite to the foliation is usually ambiguous. However, Kuhns et al. (1994) observed that in muscovite-rich rocks, kyanite grains displayed evidence of rotation in the plane of the main (S2a) foliation, which they took as evidence for growth of kyanite before (or possibly during) the main deformation during peak M1 metamorphism (see Figs. 4B–4D). Similar textures were observed in kyanite–muscovite-bearing Moose Lake porphyry samples. We make the additional observation that aggregates of aligned kyanite blades coat trains of boudins of quartz–realgar vein material. This further suggests that the kyanite formed prior to, or during, S2a deformation. A possible estimate for the age of the peak metamorphism that produced kyanite may be the 2678–2676 Ma U/Pb age from titanites in metamorphosed rocks lying outside of the ore zone (Corfu and Muir 1989b), which may have been less affected by the late, static overprint that is more pronounced in the ore zone (Kuhns et al. 1994). Magmatism at this time is indicated by the Gowan Lake pluton (2678 ± 2 Ma, U/Pb zircon; Corfu and Muir 1989a).

Pan and Fleet (1995) considered that their first episode of kyanite growth occurred prior to the intrusion of the Cedar Lake and Heron Bay plutons, and that sillimanite growth occurred at the same time as these intrusions. In addition, Pan and Fleet suggested that sigmoidal quartz–kyanite veins and pods, some showing clusters of kyanite crystals at high angles to the vein-wall margin, record a second phase of kyanite growth that occurred long after the peak of regional metamorphism. Whereas we do not dispute this possibility, we note, as did Kuhns et al. (1994), that boudinaged quartz–kyanite veins forming trains of pods behaved as rigid bodies within the ductilely deforming host rocks. In such pods, previously formed kyanite crystals, even if originally orientated at high angles to the vein margins, might be relatively unaffected by the later deformation. In addition, the selvages of the large sigmoidal kyanite-bearing quartz pod described in this study contain kyanite–staurolite-bearing assemblages, suggesting that both the veins and the selvages were subjected to amphibolite-facies metamorphism.

Interpretation and timing of andalusite

Whereas we document textures that suggest an early origin for andalusite, Kuhns et al. (1994) suggested that the rare, late idioblastic andalusite in the biotite-rich rocks from the ore zone (And2) represented late post-M2 growth as the rocks passed from the sillimanite zone into the andalusite zone (Fig. 4B). Furthermore, their interpretation is supported by the association of tremolite–actinolite (Kuhns et al. 1994), which indicates greenschist-facies conditions. Below

we present two scenarios that are consistent with the cross-cutting relationships of aluminosilicate minerals and their mineral associations.

Andalusite scenario 1

The interpretation that all andalusite is retrograde is difficult to reconcile with some of the observations of andalusite documented in our study. As noted earlier, coarse andalusite (And1) is a rare mineral in some veins and pods and within boudinaged quartz–realgar veins. Sillimanite needles crosscut (but do not replace) the margins of andalusite grains in two samples, indicating that at least some andalusite grew prior to sillimanite formation. If this sillimanite is of the same age as the rest of the sillimanite in the Hemlo deposit, it suggests that these andalusite crystals grew prior to the M2 sillimanite-forming event.

The andalusite crystals are strained and fractured, indicating that they may have developed prior to deformation. The coarse nature of the skeletal muscovite that has replaced some of the andalusite along fractures and rims contrasts with, and appears to predate, the more common fine-grained sericitic alteration that affects both andalusite and, to a lesser extent, kyanite, suggesting that the coarse muscovite may reflect a higher temperature replacement process. Furthermore, the selvages of these veins contain amphibolite-facies assemblages. These observations open the possibility that some vein-associated andalusite may have developed early in the metamorphic history. Complicating this interpretation is the observation that andalusite from these veins sometimes contains inclusions of corroded kyanite, and so must have postdated an episode of kyanite growth. We term this corroded kyanite Ky1 to distinguish it from the main generation of kyanite (Ky2).

These textures and mineral associations preclude the simple scenarios of either a single prograde sequence involving sequential growth of Ky–And–Sil, or a *P–T* path involving late retrograde growth of andalusite (although we agree with Kuhns et al. (1994) that their late idioblastic andalusite is consistent with this latter scenario). A possible explanation for the complex timing relationships between kyanite, sillimanite, and the coarse, fractured, vein-associated andalusite is that there were two discrete generations of kyanite (see *P–T* path in Fig. 4C). In this scenario, the first phase of kyanite (Ky1), found only in large quartz veins and pods in the deposit, may have been produced during the breakdown of a hydrous aluminum silicate, such as pyrophyllite. Pyrophyllite may have been produced from an early argillic alteration episode.

During continued heating, *P–T* conditions moved into the andalusite stability field, resulting in andalusite (And1) overgrowing and replacing most of the early kyanite (see Fig. 4C). To be consistent with the phase equilibria, this event must have occurred at pressures between approximately 2.5 and 4.5 GPa. Assuming there was only one episode of sillimanite growth (i.e., M2 of Kuhns et al. 1994), this Ky–And event must have predated the peak-regional metamorphism (M1) that produced the second, and main, phase of kyanite (Ky2) growth. A possible cause for such an early low-pressure metamorphic event could be the intrusion of a suite of large granodiorite plutons, including the nearby Cedar Lake and Heron Bay plutons. Radiometric age dating

of these plutons (2688–2684 Ma) suggests that they intruded the belt approximately 10 Ma prior to the peak of regional metamorphism (2678–2676 Ma) (Corfu and Muir 1989*a*, 1989*b*). This relative age relationship is supported by the fact that the Cedar Lake stock is overprinted by the regional, syn-peak-metamorphic foliation (Muir 1997; Jackson 1997).

An obvious difficulty with this suggestion is that it implies that some of the vein-associated andalusite (And1) survived the main M1 and retrograde M2 metamorphisms. We can offer no definite solution to this problem, other than to note that polymorphic transitions of aluminosilicates are known to be sluggish as shown experimentally and by numerous natural examples of metastable persistence of a lower grade Al_2SiO_5 mineral into the stability field of another (Kerrick 1990; Pattison 1992). Furthermore, the occurrence of And1 in large quartz pods may have isolated these grains from the more reactive rock matrix during later metamorphism.

Andalusite scenario 2

An alternative explanation for the vein-associated andalusite (And1) overgrown by sillimanite is that there was more than one episode of fluid-fluxed sillimanite growth. In this scenario, all of the andalusite may have formed late in the metamorphic cycle. This scenario requires the development of sillimanite during two discrete events. The first, and main, phase of sillimanite growth (Sil1) was most likely the dominant M2 event. The second phase of sillimanite growth (Sil2) would have had to have happened after further uplift moved the rocks into the andalusite field, when andalusite grew (see Fig. 4D).

An objection to this scenario might be that this implies reheating into the sillimanite stability field for which (unlike scenario 1) there is no independent evidence. This assumes that sillimanite growth is controlled by equilibrium processes (i.e., occurs within the sillimanite stability field), an assumption which may not pertain, especially for fibrolitic sillimanite formed by fluid fluxing in which kinetic effects are expected to be significant (see detailed review in Kerrick 1990, pp. 273–296). Even accepting an equilibrium model, the temperature increment required to reheat the andalusite-bearing rocks back into the sillimanite stability field might be small (e.g., only a few degrees celsius if the rocks were only just below the andalusite–sillimanite reaction). Heat advection by the metasomatizing fluids might have been sufficient to effect this small temperature rise.

Discussion

The textural and crosscutting relationships of aluminosilicates described above record a history of sequential growth that is more complex than those reported previously. Both scenarios presented above require multiple growth episodes of at least one aluminosilicate mineral. The *P–T*–time paths for both scenarios are equally feasible, and both are broadly consistent with the geological features reported by previous workers at the Hemlo mine site. Further work on this particular problem is warranted. However, we feel that andalusite scenario 1 is the more plausible alternative for the following reasons:

(1) There is no independent textural evidence to support the existence of two discrete sillimanite growth events.

(2) The generation of andalusite that occurs in deformed quartz veins (And1) is more deformed and displays substantially more advanced replacement by white mica than do neighbouring kyanite grains, or the late idioblastic andalusite documented by Kuhns et al. (1994). This suggests that quartz vein associated andalusite may have experienced more of the deformation and metamorphic history than the peak-metamorphic kyanite.

(3) Unaltered to weakly altered kyanite and staurolite occur in the alteration selvage of deformed, andalusite-bearing quartz veins. This association indicates that the vein, and its selvage, experienced moderate- to high-pressure amphibolite-facies metamorphism. It is feasible to suggest that the andalusite simply overgrew vein kyanite during retrograde metamorphism. However, with the expected higher permeability and more diverse mineral assemblage in the selvage, we would anticipate that the selvage assemblages would display at least as much alteration and deformation as the assemblages found within the veins. Rather, the opposite is true: selvage assemblages display less alteration than the vein assemblages.

## P–T conditions and P–T–time paths

Difficulties in P–T estimation

We encountered difficulties in estimating the P–T conditions of the different metamorphic events. The main problem is that, in the samples we observed, the aggregate assemblages of Ky + Grt ± St (peak metamorphism) and Sil ± Grt (later overprint) reported in previous studies (Burk et al. 1986; Kuhns et al. 1994) were never observed by us within individual domains in thin sections. In some thin sections, garnet occurred in one band, but was separated by other bands from kyanite and staurolite or sillimanite. The main difficulty was our inability to find coexisting garnet and Al$_2$SiO$_5$ minerals from a single domain, which limits the potential for geothermobarometry (absence of either phase severely limits the range of pressure-sensitive equilibria; see below). We note that this problem may reflect the focus of our study on altered rocks from the Hemlo ore zone, and may not pertain to the rocks used for geothermobarometry in the previous studies. In addition, we argue below that thermobarometry does not always provide reasonable P–T estimation.

Instead, we use mineral-assemblage constraints in a metapelitic petrogenetic grid to provide P–T estimation and to estimate P–T paths (Fig. 4). Whether or not all the rocks were actually metapelitic sediments is immaterial as long as they contain muscovite, biotite, and quartz. This approach provides good control on temperatures, but rather unconstrained pressure information, so we regard our estimates as approximate. The petrogenetic grid we use is a modified version of that of Pattison and Tracy (1991), which was constructed from consideration of the Spear and Cheney (1989) and Powell and Holland (1990) grids, both calculated from internally consistent thermodynamic data bases derived from experimental studies.

There are two particularly important reactions on the grid. The first is the reaction that marks the minimum stability of Al$_2$SiO$_5$ in Ms + Bt + Qtz-bearing rocks,

[1]   Ms + St + Chl + Qtz = Bt + Al$_2$SiO$_5$ + V
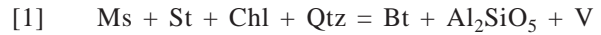
The positioning of this reaction on the grid in Fig. 4A agrees closely with the calculated position in both the Spear and Cheney (1989) and Powell and Holland (1990) grids, and agrees with available experimental constraints (Pattison 1997). The second important reaction is the model KFMASH univariant reaction,

[2]   Ms + St + Qtz = Grt + Al$_2$SiO$_5$ + Bt + V
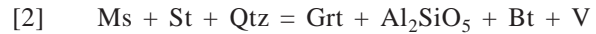
which pertains to the assemblage Ms + Qtz + Grt + Al$_2$SiO$_5$ + Bt ± St reported by Burk et al. (1986) and Kuhns et al. (1994). This reaction varies by 50°C between Spear and Cheney and Powell and Holland. We follow Pattison and Tracy (1991) in favouring the lower temperature positioning of Powell and Holland. Reaction [2] is significantly multivariant for garnets containing Mn and Ca, so we calculated the displacement of this reaction for the maximum reported combined Ca + Mn contents in garnets from kyanite- or sillimanite-bearing assemblages from Burk et al. and Kuhns et al. (XMn + XCa = 0.20). This results in a down-temperature displacement relative to the pure KFMASH system of approximately 30°C. The result is that reaction [2] is shown as a band in Fig. 4. Reaction [1], by contrast, is less affected by non-KFMASH components, the main one being Zn in staurolite which causes an up-temperature displacement.

Two potential complications in the applicability of the metapelitic grid is that it depends on the rocks containing stable Ms + Bt + Qtz, and aH$_2$O is unconstrained. In some rocks we observed, it was difficult to interpret whether or not muscovite was stable with the peak assemblage. Lack of stable muscovite invalidates the use of the grid. Regarding aH$_2$O, we consider it unlikely for aH$_2$O to have been suppressed significantly (i.e., below approx. 0.7, the composition of fluids in equilibrium with graphite at these amphibolite P–T conditions; Ohmoto and Kerrick 1977) *throughout the time of reaction* of the prograde dehydration reactions that led to the peak metamorphic assemblages; infiltration of low-aH$_2$O fluids throughout the time of reaction would be implied. This inference may not pertain to the later sillimanite overprint, which was fluid controlled, although we note that Pan and Fleet (1995) estimated that XCO$_2$ was low even in their proposed postmetamorphic calc-silicate alteration event.

P–T–time paths

The P–T paths shown in Figs. 4C and 4D correspond to the two andalusite scenarios described above. Common to the two scenarios are the P–T estimates for the peak kyanite assemblage and the later overprinting sillimanite assemblage. For the peak-metamorphic kyanite assemblage, it must lie above reaction [1] and may lie within or above the stability band for reaction [2], depending on whether or not kyanite, garnet, and staurolite coexisted in equilibrium (Burk et al. (1986) reported the stable subassemblage Grt + Ky). Our estimate shown in Figs. 4C and 4D is 6–7 GPa and 600–650°C, although higher pressures are possible from consideration of the phase equilibria alone.

Regarding the overprinting sillimanite assemblage, an argument in favour of a similar or lower temperature, rather

than a higher temperature, for this growth event is the restriction of sillimanite to knots and foliae in the rocks, indicating a lack of significant recrystallization of the matrix of the kyanite-bearing rocks to a sillimanite-bearing assemblage. This interpretation is supported by the relative *P–T* differences between the kyanite and sillimanite assemblages from the geothermobarometry of Burk et al. (1986) and our recalculation (see below) of their data (the sillimanite assemblage formed approx. 10°C and 2 GPa lower than the kyanite assemblage).

Regarding the andalusite events in scenario 1, in which we suggest there may have been early prepeak metamorphic kyanite and andalusite growth from pyrophyllite breakdown, the *P–T* conditions for this early event are constrained to between 2 and 4.5 GPa (see Fig. 4A). In scenario 2 (in which andalusite growth was generally late in the metamorphic history), all we can conclude is that it was in the andalusite stability field.

Comparison with previous metamorphic estimates

Our estimates of the *P–T* conditions of the kyanite and sillimanite assemblages, and the corresponding *P–T* path linking them, are not significantly different from those of Burk et al. (1986) and Kuhns et al. (1994) (compare Fig. 4B with Figs. 4C and 4D). The temperatures from geothermobarometry of Burk et al. are somewhat lower than we would predict from the phase equilibrium constraints (i.e., approx. 10°C below the stability of Al_2SiO_5 + Bt (reaction [1]) and approx. 40°C below Ky + Grt (reaction [2]), but, as is shown in our recalculation below, these differences are well within the combined uncertainties of the geothermobarometric methods.

Direct comparison of our results with the *P–T* estimates of Pan and Fleet (1993) is compromised by the 5–10 km separation between the two localities. Nevertheless, we consider their estimate of M1 kyanite growth of approximately 500°C and 6 GPa to be unreasonably low (approx. 100°C below the minimum stability of Al_2SiO_5 + Bt, Fig. 4B). We feel that the most likely causes for their low *P–T* estimates are either or both of the following: (*i*) the inclusion-filled garnet they used to obtain their M1 *P–T* path did not grow in a reaction involving kyanite, as they assumed, but instead grew at lower grade; and (*ii*) the biotite inclusions in the garnet reequilibrated with the garnet during cooling, leading to lower temperatures. The *P–T* estimate of Pan and Fleet for the sillimanite event is compatible with the phase equilibria.

Recalculation of geothermobarometry results of Burk et al. (1986)

We recalculated *P–T* results for the assemblages of Burk et al. (1986) using TWQ202b (Berman 1991; Berman and Aranovich 1996 data). The raw analytical data for samples B and E were obtained from Burk (1987), samples 2B-d1 to 2B-d3 and 12E-d1 to 12E-d3. The 10 mineral end members used were Pyr, Alm, Gros in garnet, An in plagioclase, Phl and Ann in biotite, Ms in muscovite, and quartz, kyanite–sillimanite, and water of unit activity, resulting in three independent equilibria in the seven-component Ca-KFMASH system. Muscovite was not analyzed, so an activity of Ms of 0.8 was assumed (typical for kyanite-grade muscovites elsewhere). The equilibria for each of the three determinations

of the sillimanite-bearing assemblage B showed tight clustering (all intersections within 30°C and 1 GPa of each other) and, as a group, ranged from 650°C and 6.3 GPa to 690°C and 7.8 GPa. In contrast, the equilibria for each of the three determinations of the kyanite-bearing assemblage E provided tight constraints on temperature but poorer clustering in pressure (typically spanning a range of 2 GPa). A loosely constrained estimate for assemblage B from these data is 700°C and 8–10 GPa. The results for the two assemblages are plotted in Fig. 4B as ellipses showing the range of the individual estimates (no estimate of the analytical and thermodynamic uncertainty is implied).

We consider that these recalculated *P–T* results are too high to reconcile with the phase equilibria (*P–T* values for two of the three determinations of the sillimanite assemblage plot in the kyanite field, and *P–T* values for all the determinations of the kyanite assemblage plot in the field of partial melting above Ms + Qtz stability; see Fig. 4B). What we find disturbing is the large difference in the absolute *P–T* values between the original geothermobarometry of Burk et al. (which was marginally too low for the phase equilibria) and the recalculated TWQ202b geothermobarometry (which is too high for the phase equilibria), considering that the same chemical data were used. We feel that this provides eloquent testimony to the importance of evaluating absolute geothermobarometry results against phase equilibrium constraints.

In contrast, the *relative* difference between the kyanite and sillimanite *P–T* results is unchanged from the original estimates of Burk et al. (1986) (the sillimanite growth event being approx. 10–40°C and 2 GPa lower than the kyanite event). This difference is consistent with the mineral assemblage constraints, and suggests that the geothermobarometry may be most useful for relative *P–T* estimation.

Implications for the metamorphic history of the Hemlo deposit and the Schreiber–Hemlo greenstone belt

One or two distinct metamorphic events?

In the absence of absolute age dating, our *P–T* results cannot unambiguously resolve the issue of whether there were two separate and distinct metamorphic episodes (an earlier kyanite event and a later sillimanite event), or whether the sillimanite event merely represents a later stage in a single metamorphic cycle. The petrological evidence used by Pan and Fleet (1993) to argue for two distinct metamorphic events was the occurrence of relict kyanite and staurolite porphyroblasts and the presence of zoning discontinuities in amphiboles and especially garnet (e.g., their Fig. 3*e*), and different *P–T* results from different parts of zoned garnet. These textures show that there were two metamorphic mineral growth episodes, with the second occurring at sufficiently different *P–T* conditions to induce some or all of consumption of previously formed minerals (e.g., kyanite and staurolite relics); new mineral growth (e.g., growth of garnet rims on earlier cores); and modification of zoning (e.g., garnet and amphibole). Whether these metamorphic growth episodes correspond to distinct metamorphic events separated by a significant period of time, or merely represent

discrete growth–reequilibration events during an evolving *P–T* path in a single metamorphic cycle, cannot be proven without direct age dating of the growth events. As discussed above, we dispute the *P–T* evidence of Pan and Fleet from zoned garnets for an early, relatively low temperature kyanite event. We find no reason to reject the suggestion of Burk et al. (1986) and Kuhns et al. (1994) of a single metamorphic cycle, with the kyanite assemblage corresponding to peak or near-peak conditions, and the later sillimanite overprint occurring during decompression. The significance of andalusite in this interpretation is discussed next.

Implications for the regional metamorphic history from andalusite relations

The two different interpretations of andalusite in our study carry rather different implications for the metamorphism of the deposit and the belt as a whole. In andalusite scenario 2, andalusite is essentially developed late in the metamorphic cycle following the main phase of sillimanite growth, and merely records the passage of the rocks through the andalusite field on the way to the surface (with the complication of a cryptic episode of late, localized sillimanite growth).

However, in the scenario that we prefer (andalusite scenario 1), a hitherto unrecognized stage of early kyanite and andalusite growth prior to the main metamorphism is implied. At the deposit, this early growth likely occurred during low-pressure metamorphism associated with intrusions of the Heron Bay – Cedar Lake suite (2688–2684 Ma, Corfu and Muir 1989*a*), which appear to have predated the main metamorphism at 2678–2676 Ma (Corfu and Muir 1989*b*). The suggestion of a preregional metamorphic growth of kyanite and andalusite may add detail to the preregional metamorphic *P–T* history of the Hemlo deposit, and therefore the eastern end of the Schreiber–Hemlo greenstone belt.

Implications for timing of gold mineralization

The three main models for the genesis of the Hemlo gold can be classified based on the relative timing of gold mineralization and regional metamorphism:

(1) *Premetamorphic*—Kuhns et al. (1994) and Johnston (1996) proposed that the Hemlo deposit originated as a Au–Mo porphyry system probably related to the intrusion of the Moose Lake porphyry complex. This interpretation is based on the metal association of Au, Mo, and epithermal-associated elements, the spatial association of the ore zones with certain phases of the Moose Lake porphyry complex, the zonation of alteration around the Moose Lake porphyry complex, the metamorphism and folding of the alteration and ore zones, and the fact that the ore bodies are cut by deformed felsic dykes, containing fragments of mineralized and altered rock, that are interpreted to be associated either with the Cedar Lake pluton (Kuhns et al. 1994) or late-stage magmatism associated with the Moose Lake porphyry (Johnston 1996).

(2) *Syn- to late metamorphic*—Many investigators, including Burk et al. (1986), Hugon (1986), and Corfu and Muir (1989*a*, 1989*b*), concluded that the Hemlo deposit is a shear-zone-related deposit that formed by precipitation of metals from a metamorphic fluid during, or shortly after, regional metamorphism. This interpretation is based on the association of mineralization with zones of high strain within the metamorphic terrain, the presence of syntectonic gold-bearing veins, the association of amphibolite-facies silicate minerals with gold in some quartz veins, and late- to postmetamorphic age dates from minerals associated with mineralization.

(3) *Postmetamorphic*—Pan and Fleet (1993, 1995) suggested that Au mineralization at Hemlo occurred approximately 40 million years after regional metamorphism. Their interpretation is based on the occurrence of the deposit within the Hemlo shear zone, occurrence of some gold in zones of postmetamorphic, medium- to low-grade calc-silicate alteration zones (but see Kuhns et al. 1995), late overprinting by sulphide minerals, and the abundance of ostensibly low temperature As-, Hg-, Tl-, and Sb-bearing minerals associated with Au mineralization.

Studies on the mineral assemblages and textures of both silicate and sulphide minerals, including this study and that of Powell and Pattison (1997), carry implications for the timing of mineralization relative to metamorphism. One of the boudinaged andalusite-bearing veins (with a kyanite-bearing vein selvage) contains realgar and stibnite and displays a conspicuous halo of realgar. Thus, there is little question that the vein was emplaced after, or during, As–Sb mineralization, and prior to metamorphism and deformation. Based on the exsolution history of As–Hg–Sb sulphides, Powell and Pattison suggested that these metals (along with gold) had experienced moderate to high temperatures, thereby suggesting pre- to synmetamorphic mineralization. If our preferred andalusite scenario 1 (early andalusite) is correct, then the association of early andalusite with mineralized quartz veins requires that gold and other metals were emplaced prior to regional metamorphism.

Many of the features documented by researchers supporting a syn- or postmetamorphic origin for the gold mineralization, such as those listed by Hugon (1986) and Pan and Fleet (1995), can be accounted for by subsequent deformation, metamorphic recrystallization, and hydrothermal remobilization of a preexisting deposit. For example, direct associations between gold grains and kyanite in quartz veins (Hugon 1986; Harris 1989; Pan and Fleet 1995), and between gold grains and late-stage, low-temperature calc-silicate minerals (Pan and Fleet 1995), do not necessarily indicate that the kyanite vein- and calc-silicate-forming events were responsible for the introduction of gold. An equally valid explanation (Kuhns et al. 1994) is that the gold was already in the rock, and was simply remobilized by these events. Powell and Pattison (1997) provided evidence for millimetre- to centimetre-scale remobilization of gold and other metals in the deposit. The location of the deposit within deformed and metamorphosed rocks of the Hemlo shear zone, and the coincidence of several phases of alteration and possibly mineralization, may reflect prolonged exploitation of a major structure by both magmas and hydrothermal fluids (Kuhns et al. 1995).

Acknowledgments

References

Bégin, N.J. 1992. Contrasting mineral isograd sequences in metabasites of the Cape Smith Belt, northern Quebec, Canada: three new bathograds for mafic rocks. Journal of Metamorphic Geology, **10**: 685–704.

Berman, R.G. 1991. Thermobarometry using multiequilibrium calculations: a new technique with petrologic applications. Canadian Mineralogist, **29**: 833–855.

Berman, R.G., and Aranovich, L.Y. 1996. Optimized standard state and mixing properties of minerals: I. Model calibration for olivine, orthopyroxene, cordierite, garnet and ilmenite in the system $FeO–MgO–CaO–Al_2O_3–SiO_2–TiO_2$. Contributions to Mineralogy and Petrology, **126**: 1–24.

Burk, R.R. 1987. Geological setting of the Teck–Corona gold–molybdenum deposit, Hemlo, Ontario. M.A.Sc. thesis, Queen's University, Kingston, Ont.

Burk, R., Hodgson, C.J., and Quartermain, R.A. 1986. The geological setting of the Teck–Corona Au–Mo–Ba deposit, Hemlo, Ontario, Canada. *In* Gold'86. *Edited by* A.J. MacDonald. Konsult International, Willowdale, Ont., pp. 311–326.

Carmichael, D.M. 1969. On the mechanism of prograde metamorphic reactions in quartz-bearing pelitic rocks. Contributions to Mineralogy and Petrology, **20**: 244–267.

Corfu, F., and Muir, T.L. 1989a. The Hemlo – Heron Bay greenstone belt and Hemlo Au–Mo deposit, Superior Province, Ontario, Canada: 1. Sequence of igneous activity determined by zircon U–Pb geochronology. Chemical Geology, **79**: 183–200.

Corfu, F., and Muir, T.L. 1989b. The Hemlo – Heron Bay greenstone belt and Hemlo Au–Mo deposit, Superior Province, Ontario, Canada: 2. Timing of metamorphism, alteration and Au mineralization from titanite, rutile and monazite U–Pb geochronology. Chemical Geology, **79**: 201–223.

Couture, J.F., Pilote, P., Machado, N., and Desroches, J.P. 1994. Timing of gold mineralization in the Val d'Or district, southern Abitibi belt: evidence for two distinct mineralizing events. Economic Geology, **89**: 1542–1551.

Eugster, H.P. 1970. Thermal and ionic equilibria among muscovite, K-feldspar and aluminosilicate assemblages. Fortschritte der Mineralogie, **47**: 106–123.

Fleet, M.E., and Pan, Y. 1995. Magmatism, metamorphism and deformation at Hemlo, Ontario, and the timing of Au–Mo mineralization in the Golden Giant mine – A discussion. Economic Geology, **90**: 1338–1341.

Fleet, M.E., Seller, M.H., and Pan, Y. 1997. Rare earth elements, protoliths and alteration at the Hemlo gold deposit, Ontario, Canada, and comparison with argillic and sericitic alteration in the Highland Valley Porphyry district, British Columbia, Canada. Economic Geology, **92**: 551–568.

Grant, J.W. 1995. $^{40}Ar/^{39}Ar$ geochronology of the post-metamorphic thermal history of the Hemlo area. M.Sc. thesis, Queen's University, Kingston, Ont.

Harris, D.C. 1989. The mineralogy and geochemistry of the Hemlo gold deposit, Ontario. Geological Survey of Canada, Economic Geology Report 38.

Heaman, L.M., and Parrish, R. 1991. U–Pb geochronology of accessory minerals. *In* Applications of radiometric isotope systems to problems in geology. *Edited by* L. Heaman and J.N. Ludden. Mineralogical Association of Canada Short Course 19, pp. 59–102.

Hugon, H. 1986. The Hemlo deposits, Ontario, Canada: a central portion of a large scale, wide zone of heterogeneous ductile shear. *In* Gold'86. *Edited by* A.J. MacDonald. Konsult International, Willowdale, Ont., pp. 379–387.

Jackson, S.L. 1997. Patterns of structure and metamorphism in the Hemlo greenstone belt. 43rd Annual Institute on Lake Superior Geology, Vol. 43, Part 1, pp. 27–28.

Johnston, P. 1996. Geological setting of the Hemlo gold deposit, Ontario, Canada. Ph.D. thesis, Queen's University, Kingston, Ont.

Kerrick, D.M. 1990. The Al_2SiO_5 polymorphs. Reviews in Minerology No. 22.

Kretz, R. 1983. Symbols for rock-forming minerals. American Mineralogist, **68**: 277–279.

Kuhns, R.J. 1986. Alteration styles and trace element dispersion associated with the Golden Giant deposit, Hemlo, Ontario, Canada. *In* Gold'86. *Edited by* A.J. MacDonald. Konsult International, Willowdale, Ont., pp. 340–354.

Kuhns, R.J., Sawkins, F.J., and Ito, E. 1994. Magmatism, metamorphism and deformation at Hemlo, Ontario, and the timing of Au–Mo mineralization in the Golden Giant mine. Economic Geology, **89**: 720–756.

Kuhns, R.J., Sawkins, F.J., and Ito, E. 1995. Magmatism, metamorphism and deformation at Hemlo, Ontario, and the timing of Au–Mo mineralization in the Golden Giant mine – A reply. Economic Geology, **90**: 1343–1344.

Michibayashi, K. 1995. Two phase syntectonic gold mineralization and barite remobilization within the main ore body of the Golden Giant mine, Hemlo, Ontario, Canada. Ore Geology Reviews, **10**: 31–50.

Morasse, M., Wasteneys, H.A., Cormier, M., Helmstaedt, H., and Mason, R. 1995. A pre-2686 Ma intrusion-related gold deposit in the Kiena mine, Val d'Or, Quebec, southern Abitibi province. Economic Geology, **90**: 1310–1320.

Muir, T.L. 1993. The geology of the Hemlo gold deposit area. Ontario Geological Survey, Open File Report 5877.

Muir, T.L. 1997. Precambrian geology of the Hemlo gold deposit area. Ontario Geological Survey, Report 289.

Ohmoto, H., and Kerrick, D. 1977. Devolatilization equilibria in graphitic systems. American Journal of Science, **277**: 1031–1044.

Pan, Y., and Fleet, M.E. 1993. Polymetamorphism in the Archean Hemlo – Heron Bay greenstone belt, Superior Province: *P–T* variations and implications for tectonic evolution. Canadian Journal of Earth Sciences, **30**: 985–996.

Pan, Y., and Fleet, M.E. 1995. The late Archean Hemlo gold deposit, Ontario, Canada: a review and synthesis. Ore Geology Reviews, **9**: 455–488.

Pattison, D.R.M. 1992. Stability of andalusite and sillimanite and the Al_2SiO_5 triple point: constraints from the Ballachulish aureole, Scotland. Journal of Geology, **100**: 423–446.

Pattison, D.R.M. 1997. Are metapelitic Al_2SiO_5 assemblages stable? In most cases, probably not. Geological Association of Canada, Program with Abstracts, **22**: A113.

Pattison, D.R.M., and Tracy, R.J. 1991. Phase equilibria and thermobarometry of metapelites. *In* Contact metamorphism.

Edited by D.M. Kerrick. Reviews in Minerology No. 25, pp. 105–206.

Powell, R., and Holland, T. 1990. Calculated mineral equilibria in the pelitic system, KFMASH (K_2O–FeO–MgO–Al_2O_3–SiO_2–H_2O). American Mineralogist, **75**: 367–380.

Powell, W.G., and Pattison, D.R.M. 1997. An exsolution origin for "low-temperature" sulphides at the Hemlo Gold Deposit, Ontario, Canada. Economic Geology, **92**: 569–577.

Powell, W.G., Carmichael, D.M., and Hodgson, C.J. 1995. Conditions and timing of metamorphism in the southern Abitibi greenstone belt, Quebec. Canadian Journal of Earth Sciences, **32**: 787–805.

Robert, F., and Brown, A.C. 1986. Archean gold-bearing quartz veins at the Sigma mine, Abitibi greenstone belt, Quebec: Part I. Geological relations and formation of the vein system. Economic Geology, **81**: 578–592.

Scott, D.A., and St-Onge, M.A. 1995. Constraints on Pb closure temperature in titanite based on rocks from the Ungava orogen, Canada: implications for U–Pb geochronology and *P–T–t* path determinations, Geology, **23**: 1123–1126.

Spear, F.S., and Cheney, J.T. 1989. A petrogenetic grid for pelitic schists in the system SiO_2–Al_2O_3–FeO–MgO–K_2O–H_2O. Contributions to Mineralogy and Petrology, **101**: 149–164.

Vernon, R.H. 1979. Formation of late sillimanite by hydrogen metasomatism (base-leaching) in some high-grade gneisses. Lithos, **12**: 143–152.

Walford, P., Stephens, J., Skrecky, G., and Barnett, R. 1986. The geology of the 'A' zone, Page–Williams mine, Hemlo, Ontario, Canada. *In* Gold'86. *Edited by* A.J. MacDonald. Konsult International, Willowdale, Ont., pp. 362–378.

Williams, H.R., Stott, G.M., Heather, K.B., Muir, T.L., and Sage, R.P. 1991. Wawa subprovince. *In* Geology of Ontario. *Edited by* P.C. Thurston, H.R. Williams, R.H. Sutcliffe, and G.M. Stott. Ontario Geological Survey, Special Volume 4, Part 1, pp. 485–539.

Wintsch, R.P., and Andrews, M.S. 1988. Deformation-induced growth of sillimanite: "stress" minerals revisited. Journal of Geology, **96**: 143–161.